Regulation of Kif15 localization and motility by the C-terminus of TPX2 and microtubule dynamics

Barbara J. Mann†, Sai K. Balchand†, and Patricia Wadsworth*
Department of Biology and Program in Molecular and Cellular Biology, University of Massachusetts Amherst, Amherst, MA 01003

ABSTRACT **Mitotic motor proteins generate force to establish and maintain spindle bipolarity, but how they are temporally and spatially regulated in vivo is unclear. Prior work demonstrated that a microtubule-associated protein, TPX2, targets kinesin-5 and kinesin-12 motors to spindle microtubules. The C-terminal domain of TPX2 contributes to the localization and motility of the kinesin-5, Eg5, but it is not known whether this domain regulates kinesin-12, Kif15. We found that the C-terminal domain of TPX2 contributes to the localization of Kif15 to spindle microtubules in cells and suppresses motor walking in vitro. Kif15 and Eg5 are partially redundant motors, and overexpressed Kif15 can drive spindle formation in the absence of Eg5 activity. Kif15-dependent bipolar spindle formation in vivo requires the C-terminal domain of TPX2. In the spindle, fluorescent puncta of GFP-Kif15 move toward the equatorial region at a rate equivalent to microtubule growth. Reduction of microtubule growth with paclitaxel suppresses GFP-Kif15 motility, demonstrating that dynamic microtubules contribute to Kif15 behavior. Our results show that the C-terminal region of TPX2 regulates Kif15 in vitro, contributes to motor localization in cells, and is required for Kif15 force generation in vivo and further reveal that dynamic microtubules contribute to Kif15 behavior in vivo.**

Monitoring Editor
Yixian Zheng
Carnegie Institution

Received: Jun 30, 2016
Revised: Nov 4, 2016
Accepted: Nov 7, 2016

INTRODUCTION

During mitosis, microtubules are nucleated and organized into a dynamic structure called the mitotic spindle, which mediates chromosome segregation into two daughter cells. In mammalian cells, microtubule nucleation at centrosomes, near chromatin, and from preexisting microtubules all contribute to spindle formation (Meunier and Vernos, 2016). Microtubule formation near chromatin and at kinetochores is regulated by nuclear localization sequence containing spindle assembly factors that are inactive when bound to importins α/β (Gruss and Vernos, 2004). The small GTPase Ran, which is locally activated near chromatin (Kalab *et al.*, 2006), binds to importin β and relieves this inhibitory effect, thus promoting microtubule formation. A well-studied Ran-regulated spindle assembly factor is TPX2, which stimulates microtubule formation at kinetochores and in the chromatin region and is required for spindle assembly and completion of mitosis (Tulu *et al.*, 2006; O'Connell *et al.*, 2009).

During spindle formation the duplicated centrosomes separate to establish spindle bipolarity. Centrosome separation is driven by the kinesin-5, Eg5, a bipolar, tetrameric motor that cross-links and slides antiparallel microtubules (Kapitein *et al.*, 2005; Ferenz *et al.*, 2010). More recently, it was shown that after bipolar spindle formation, the action of Eg5 is dispensable, and spindle bipolarity is maintained by a kinesin-12, Kif15 (Tanenbaum *et al.*, 2009; Vanneste *et al.*, 2009). Spindles in cells depleted of Kif15 are shorter than spindles in control cells, consistent with a model in which Kif15, like Eg5, generates outward force in the spindle (Sturgill and Ohi, 2013). However, in contrast to Eg5, Kif15 preferentially associates with kinetochore fiber microtubules. Cells overexpressing

This article was published online ahead of print in MBoC in Press (http://www.molbiolcell.org/cgi/doi/10.1091/mbc.E16-06-0476) on November 16, 2016.

†These authors contributed equally.

B.J.M. and S.K.B. performed molecular cloning, protein purification, and single-molecule experiments. S.K.B. and P.W. performed live imaging. B.J.M. performed image quantification. P.W. prepared the GFP-Kif15 cell line and designed the experiments. P.W. wrote the manuscript with the assistance of B.J.M. and S.K.B.

*Address correspondence to: P. Wadsworth (patw@bio.umass.edu).

Abbreviations used: FCPT, 2-[1-(4-fluorophenyl)cyclopropyl]-4-(pyridin-4-yl)thiazole; STLC, *S*-trityl-L-cysteine.

Kif15 can form a bipolar spindle in the absence of Eg5 activity (Tanenbaum *et al.*, 2009; Raaijmakers *et al.*, 2012; Sturgill and Ohi, 2013). The existence of two mitotic motors that can each power bipolar spindle formation may contribute to the lack of efficacy of Eg5 inhibitors in clinical trials, and understanding how these motors are regulated therefore may be of clinical significance (Waitzman and Rice, 2014).

Localization of kinesin-12 and kinesin-5 motors to spindle microtubules requires TPX2 (Tanenbaum *et al.*, 2009; Vanneste *et al.*, 2009; Ma *et al.*, 2011). In fact, TPX2 was initially discovered as a factor required for the dynein-dependent targeting of the *Xenopus* kinesin-12, Xklp2, to spindle poles (Wittmann *et al.*, 1998). The C-terminal 37 amino acids of TPX2 are required to target Eg5 to the spindle; targeting of Kif15 requires the C-terminal leucine zipper of the motor (Wittmann *et al.*, 1998). The C-terminal half of TPX2 is required to localize Kif15 to the spindle (Brunet *et al.*, 2004), but it was not known whether a specific domain of the protein is necessary.

These initial studies on TPX2 and Kif15 were consistent with the idea that dimers of Kif15 walked along one microtubule while tethered to a second microtubule via TPX2, thus generating force for spindle formation (Vanneste *et al.*, 2009). Subsequently Sturgill *et al.* (2014) provided biochemical data showing that the motor was an autoinhibited dimer and identified a second, nonmotor microtubule-binding site in the coil 1 region of Kif15. These data led to a model in which autoinhibited Kif15 dimers were first unmasked and then bound to microtubule bundles via motor and nonmotor binding sites (Sturgill *et al.*, 2014). More recent work, however, showed that Kif15 exists as a tetramer that displays processive motility along individual microtubules in vitro (Drechsler *et al.*, 2014; Drechsler and McAinsh, 2016). Thus the oligomeric state of Kif15 and how it contributes to mitotic spindle formation remain unresolved. Finally, experiments using dynamic microtubules in vitro show that Kif15 accumulates at microtubule plus ends, suppresses catastrophe events, and can cross-link microtubules and move them relative to one another, promoting the formation of parallel microtubule arrays (Dreschler and McAinsh, 2016). Thus both Eg5 and Kif15 contribute to spindle bipolarity and are regulated by TPX2, but their mechanisms of action are distinct.

To gain insight into the cellular function and regulation of the kinesin-12, Kif15, we investigated the behavior of the motor and its regulation by TPX2 in vitro and in vivo. Our data show that Kif15 motors, present in diluted mammalian cell extracts, are processive, track-switching tetramers and that the C-terminal region of TPX2 is required to inhibit Kif15 motor stepping. Using a knockdown-rescue approach in mammalian cells, we further demonstrate that the C-terminal region of TPX2 contributes to targeting the motor to the mitotic spindle and that Eg5-independent bipolar spindle formation by overexpressed Kif15 requires the TPX2 C-terminal region. In live cells, GFP-Kif15 displays robust, plus end–directed motility at a rate similar to that of microtubule growth, and this behavior is suppressed by paclitaxel. Together these results document the behavior of Kif15 in cells and demonstrate the importance of TPX2 and its C-terminal region for motor localization and activity.

RESULTS

TPX2 C-terminus contributes to Kif15 targeting to spindle microtubules

The C-terminal 37 amino acids of TPX2 contribute to the targeting of the kinesin-5, Eg5, to spindle microtubules (Ma *et al.*, 2011), but it is not known whether this domain contributes to the targeting of the kinesin-12, Kif15, to the spindle (Wittmann *et al.*, 1998; Brunet *et al.*, 2004; Tanenbaum *et al.*, 2009; Vanneste *et al.*, 2009). To address this, we first examined the distribution of endogenous Kif15 in LLC-Pk1 cells expressing full-length TPX2 or TPX2-710, which lacks the C-terminal 37 amino acids, from bacterial artificial chromosomes (BACs) and depleted of the endogenous protein using small interfering RNA (siRNA; Ma *et al.*, 2011). Cells were fixed and stained for microtubules and Kif15 at 40 h after nucleofection with TPX2 siRNA, a time when the majority of TPX2 is depleted (Supplemental Figure S1A; Ma *et al.*, 2011). Kif15 was present along spindle microtubules in parental LLC-Pk1 cells but not in parental cells depleted of TPX2 (Figure 1A). In LLC-Pk1 cells expressing full-length TPX2 or TPX2-710 from a BAC and depleted of endogenous TPX2, Kif15 was detected on spindle microtubules when full-length TPX2 was present and was reduced when TPX2-710 was expressed (Figure 1A). Quantification of the ratio of Kif15 to microtubules at the spindle pole and in the spindle midway between the chromosomes and pole shows a statistically significant reduction at both locations in cells expressing TPX2-710 compared with cells expressing full-length TPX2 (Figure 1C). As previously reported (Ma *et al.*, 2011), expression of TPX2-710 in cells depleted of TPX2 resulted in aberrant spindle morphology (Figure 1B). These results demonstrate that for both Eg5 and Kif15, the C-terminal domain of TPX2 contributes to spindle targeting.

Full-length TPX2 inhibits Kif15 motor velocity

Next we sought to determine whether the C-terminal domain of TPX2 was required to regulate Kif15 motor stepping in vitro. To do this, we transfected LLC-Pk1 cells with full-length Kif15 tagged with enhanced green fluorescent protein (GFP-Kif15; Vanneste *et al.*, 2009) and used these cells to prepare cytoplasmic extracts for use in single-molecule total internal reflection fluorescence (TIRF) microscopy experiments (Figure 2A; Cai *et al.*, 2007; Balchand *et al.*, 2015). Rhodamine-labeled, paclitaxel-stabilized microtubules were attached to the surface of a microscope flow chamber, and cell extract diluted in motility buffer was added (*Materials and Methods*). Fluorescent puncta were observed to bind to microtubules and processively move upon addition of ATP (Figure 2, B, C, and G). Of note, nearly every GFP-Kif15 puncta that bound a microtubule was motile, demonstrating that Kif15 from mammalian cells is not autoinhibited (Sturgill *et al.*, 2014) but displays robust motility. TPX2 is undetectable in these cytoplasmic extracts because they are prepared from asynchronous cells, >95% of which are in interphase, a time when TPX2 is located in the nucleus (Balchand *et al.*, 2015).

GFP-Kif15 was observed to move predominantly in a plus end–directed manner (86% of events), with a smaller percentage of events toward the minus end (see *Materials and Methods*; 14% of events; Drechsler *et al.*, 2014; Figure 2B). The average velocity of plus end–directed motion was 128.7 nm/s, and the velocity of minus end–directed motion was slower, 86.6 nm/s. Motility was processive, with average run lengths of 1.9 and 0.9 μm in the plus- and minus-end directions, respectively (Figure 2B). In addition to directional reversals, Kif15 motors moving on one microtubule could switch to a neighboring microtubule and continue processive motility (Figure 2C). In extracts prepared from LLC-Pk1 cells arrested in mitosis with a low concentration of nocodazole (*Materials and Methods*), motor velocity (151 nm/s, $n = 54$, 53 plus-end directed and 1 minus-end directed) was not different from that measured in interphase, with the caveat that TPX2 is present in these extracts. Of interest, minus end–directed motility was reduced in the mitotic compared with the interphase extract. These data suggest that in in vitro assays, motor microtubule affinity is sufficiently strong to overcome any potential mitotic regulation (vanHeesbeen *et al.*, 2016). This possibility is consistent with the observation that Eg5 prepared

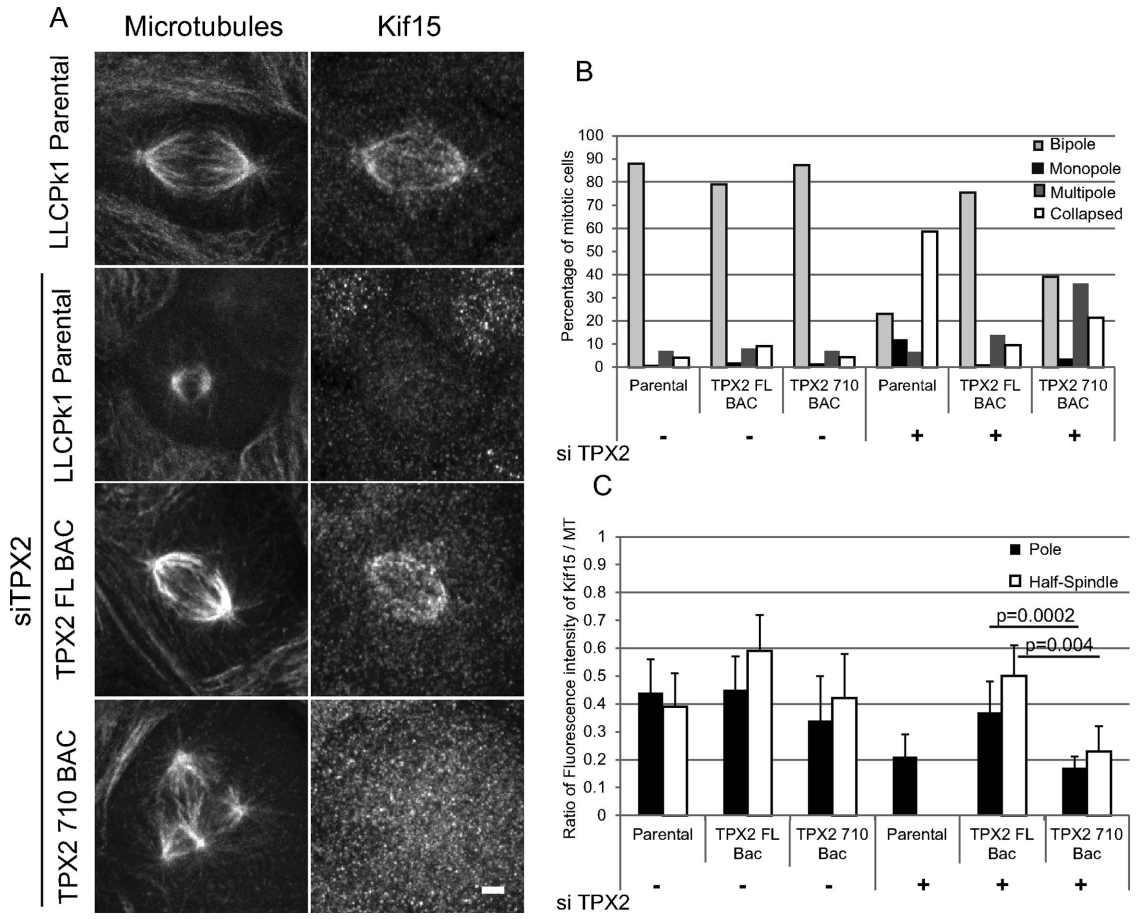

FIGURE 1: The C-terminal region of TPX2 contributes to spindle localization of Kif15. (A) Immunofluorescence staining for microtubules (left) and Kif15 (right). Top, parental cells; the remaining three rows show cells depleted of TPX2 and expressing no transgene (parental), transgene encoding full-length TPX2 (middle), or TPX2-710 (bottom). Scale bar, 2 μm. (B) Spindle morphology for parental cells and cells expressing full-length or truncated TPX2; cells on the right were additionally treated with siRNA targeting TPX2. (C) Quantification of fluorescence ratio of Kif15 to tubulin at pole and in the half-spindle. Error bars are SD. Parental cells depleted of TPX2 were only measured at spindle pole due to loss of spindle microtubules.

from interphase extracts, and thus lacking the mitosis-specific phosphorylation that is required for spindle microtubule binding (Blangy *et al.*, 1995), shows robust motility in vitro (Balchand *et al.*, 2015).

Kif15 was previously reported to exist as a tetramer or dimer using purified motors (Drechsler *et al.*, 2014; Sturgill *et al.*, 2014) or motors in mammalian cell extracts (Dreschler and McAinsh, 2016; Sturgill *et al.*, 2016). Understanding the quaternary structure of the molecule is significant because tetramers can potentially interact with more than one microtubule simultaneously and formation of tetramers could potentially alter the availability of a second microtubule-binding site in the motor tail (Sturgill *et al.*, 2014). To determine the oligomeric state of GFP-Kif15 in our experiments, we acquired images of purified kinesin-1-GFP, which is known to be a dimer, and GFP-Kif15 using identical imaging conditions and using only motors that bound to microtubules. For this experiment, endogenous Kif15 was depleted from the cells before preparation of the extract, so that the motors would be composed predominantly of the expressed GFP-tagged protein (Supplemental Figure S1B). As shown in the histogram in Figure 2D, bottom), Kif15 puncta showed a range of fluorescence intensities, with an average intensity that was 1.6 times the average fluorescence intensity of kinesin-1–GFP (Figure 2D, top; average fluorescence of 220.5 and 141.0 arbitrary units). The reason that the average value was not twice the intensity of kinesin-1-GFP may result from incomplete depletion of endogenous Kif15 by siRNA (Supplemental Figure 1B), resulting in a mixture of motors containing two, three, or four GFP-tagged motors. In addition, some motors may dissociate into dimers during preparation (Drechsler *et al.*, 2014; Sturgill *et al.*, 2014, 2016). We also imaged GFP-Kif15 in the absence of ATP and counted bleach steps. We observed at least three discrete bleach events for approximately half of the particles (Figure 2E), consistent with at least some of the GFP-Kif15 existing as a tetramer under these conditions. To determine whether Kif15 exists as a tetramer in mitosis, we added mitotic extract to microtubules in chambers without ATP and counted the number of bleach steps. In this experiment, we observed particles with greater than three bleach steps for more than half of the particles (Figure 2E), demonstrating that in both interphase and mitotic extracts, some of the Kif15 motors exist as tetramers.

In summary, these data show that GFP-Kif15, prepared from mammalian cells, moves rapidly and processively toward microtubule plus ends and can both switch microtubule tracks and reverse direction. The motile parameters of Kif15 prepared from mammalian cells are strikingly similar to motors purified from Sf9 cells and indicate that the native state of Kif15 in interphase and mitotic mammalian

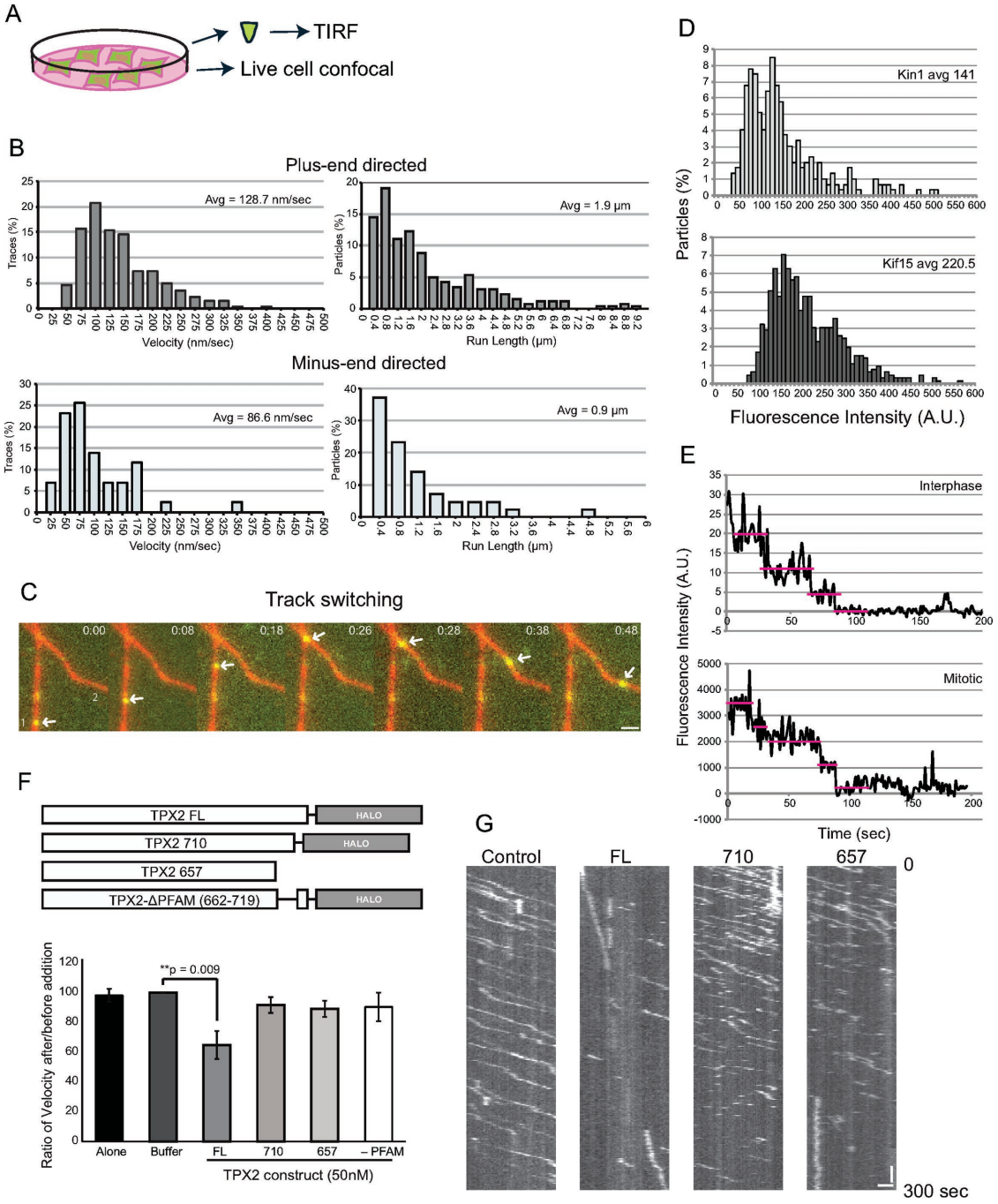

FIGURE 2: Inhibition of Kif15 motor stepping requires full-length TPX2. (A) Schematic diagram of experiment. (B) Histograms of GFP-Kif15 velocity (left) and run length (right) for plus end– and minus end–directed motion; $n = 261$ and 43 motors, respectively. Data from two independent experiments. (C) GFP-Kif15 switches microtubule tracks; arrow marks moving GFP-Kif15 puncta. Time in minutes:seconds. Bar, 1 µm. (D) Histogram of fluorescence intensity of kinesin-1–GFP (top) and GFP-Kif15 (bottom); fluorescence in arbitrary units (A.U.). For kinesin-1–GFP, $n = 295$, and for GFP-Kif15, $n = 652$, from two independent experiments. (E) Photobleaching of microtubule-bound GFP-Kif15 from interphase and mitotic extracts. Horizontal pink lines show bleach steps. For interphase, $n = 11$ particles, five with more than three steps and six with fewer than three steps; data from two independent experiments; for mitotic extracts, $n = 15$ particles, 10 with more than three steps and five with fewer than three steps. (F) Schematic diagram of constructs used for inhibition experiments (top) and bar graph (bottom) showing ratio of velocity without and with added proteins; error bars, SEM. (G) Kymographs showing motility of GFP-Kif15; added TPX2 construct indicated at the top; vertical axis marker bar, 15 s; horizontal axis marker bar, 1 µm.

cells is likely a tetramer (Drechsler *et al.*, 2014) that can dissociate into dimers depending on the experimental conditions (Drechsler *et al.*, 2014; Dreschler and McAinsh, 2016; Sturgill *et al.*, 2014, 2016).

To identify the region, or regions, of TPX2 that regulate Kif15 motility in vitro, we incubated TPX2 with diluted extract containing GFP-Kif15 and then introduced it into the motility chamber. When

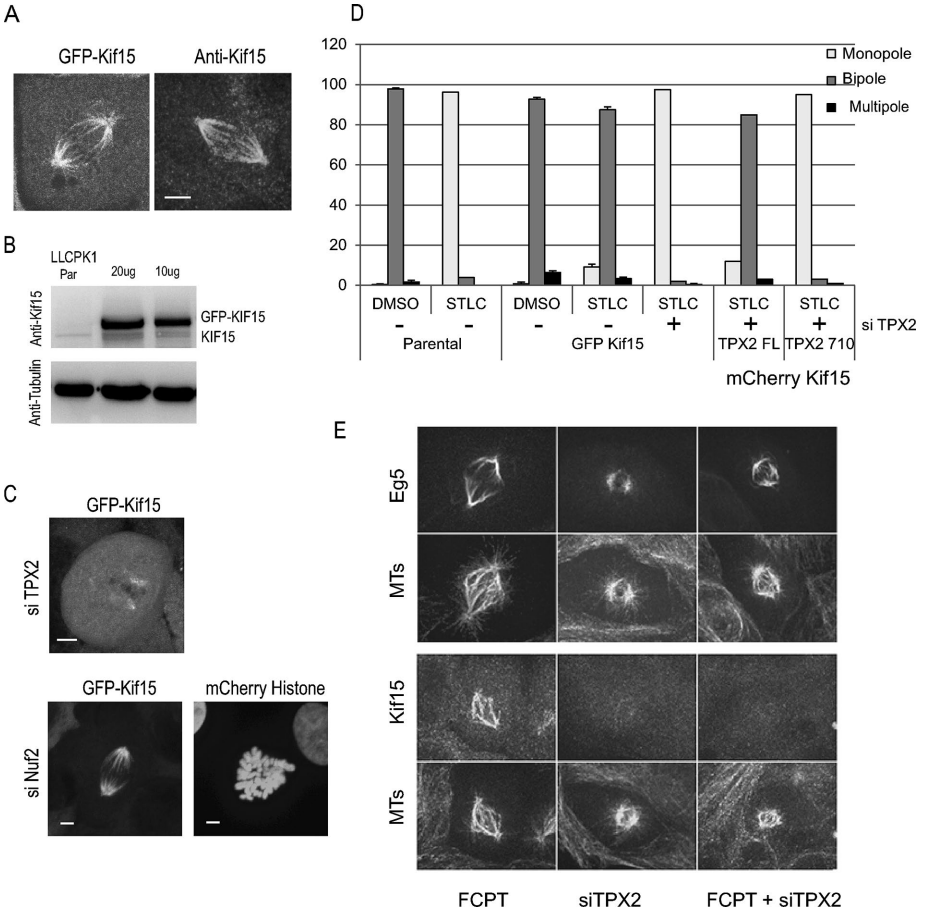

FIGURE 3: TPX2 is required for bipolar spindle formation in cells overexpressing Kif15. (A) LLC-Pk1 cells expressing GFP-Kif15 (left) and parental cells fixed and stained for Kif15 (right). (B) Western blot of extracts from parental and GFP-Kif15–expressing cells; blot stained for Kif15 (top) and tubulin as loading control (bottom). (C) Images of GFP-Kif15–expressing cells treated with siRNA targeting TPX2 (top) or Nuf2 (bottom); GFP-Kif15 (left) and co-nucleofected mCherry-H2B to label chromosomes (right). (D) Bar graphs showing percentage of bipolar, monopolar, and multipolar spindles for each treatment condition. Error bars show SD. (E) Parental cells treated with FCPT, with siRNA targeting TPX2, or with both. Cells were stained for microtubules (bottom) and either Kif15 or Eg5 (top). Bar, 2 μm.

full-length TPX2 was present in the reaction, motor velocity was reduced to ~65% of controls (Figure 2, F and G). Next we added TPX2-710, which binds microtubules (Balchand *et al.*, 2015) and contributes to motor targeting (Figure 1), to determine whether it also regulates motility in vitro. Incubation of TPX2-710 with GFP-Kif15 before addition to the motility chamber did not result in a statistically significant reduction in motor velocity (Figure 2, F and G) demonstrating that full-length TPX2 is required for motor inhibition. Two additional constructs, one lacking a larger C-terminal region (TPX2-657) and one containing a deletion of a conserved PFAM domain near the C-terminus (TPX2-ΔPFAM; Supplemental Figure S1C), also failed to inhibit Kif15 (Figure 2, F and G). The lack of inhibition with the ΔPFAM construct, which is missing only part of the region deleted in TPX2-710, indicates that these nine amino acids may play a role in motor inhibition. Both TPX2-657 and TPX2-ΔPFAM bound microtubules after expression in mammalian cells depleted of endogenous TPX2 (Supplemental Figure S1D), demonstrating that failure to inhibit Kif15 did not result from failure of these proteins to bind microtubules. In summary, these experiments show that full-length TPX2 is required to inhibit Kif15 motor stepping in vitro.

TPX2 is required for bipolar spindle formation in cells overexpressing Kif15

Previous work showed that bipolar spindle formation can proceed in cells lacking Eg5 activity and overexpressing Kif15, demonstrating that Kif15 can generate force for spindle formation in vivo (Tanenbaum *et al.*, 2009; Sturgill and Ohi, 2013). To understand how TPX2 contributes to Kif15-dependent spindle formation in vivo, we examined spindle formation in LLC-Pk1 cells overexpressing GFP-Kif15. In these cells, the distribution of GFP-Kif15 on spindle microtubules was similar to the distribution of Kif15 in the parental cells, showing a punctate staining pattern with enrichment along kinetochore fiber microtubules and near spindle poles (Figure 3A). This distribution is equivalent to that observed in *Xenopus* cultured cell spindles (Wittmann *et al.*, 2000) and similar to the distribution in other cultured mammalian cells (Tanenbaum *et al.*, 2009; Vanneste *et al.*, 2009; Sturgill and Ohi, 2013). Western blots of an extract of GFP-Kif15 cells show that GFP-Kif15 is present at approximately 10 times the level of endogenous Kif15 in the parental cells (*Materials and Methods*; Figure 3B).

First, we asked whether TPX2 is required for Kif15 localization in overexpressing cells. Treatment with siRNA targeting TPX2 resulted in a dramatic reduction in GFP-Kif15 on spindle microtubules and an ensuing increase in the level of cytoplasmic fluorescence (Figure 3C). In some cells, residual GFP-Kif15 was detected near spindle poles (Figure 3C). These results demonstrate that TPX2 contributes to the localization of GFP-Kif15 to spindle microtubules, even when high levels of the motor are present.

In control cells, Kif15 is enriched on kinetochore fiber microtubules (Sturgill and Ohi, 2013) and when overexpressed Kif15 binds and stabilizes nonkinetochore microtubules as well, where it is believed to play a key role in Eg5-independent spindle formation (Sturgill and Ohi, 2013). We asked whether kinetochore fiber microtubules are needed for Kif15 localization in LLC-Pk1 GFP-Kif15 cells. In cells depleted of Nuf2, a treatment that prevents kinetochore fiber formation (Supplemental Figure S2), GFP-Kif15 remained associated with the spindle (Figure 3C, left) despite the loss of kinetochore fibers and concomitant failure of chromosome congression (Figure 3C, right). We also tested the requirement for kinetochore fibers for Kif15 localization in parental cells by depleting Nuf2 and staining for Kif15 (unpublished data); in these cells, the spindle localization of Kif15 is reduced but not completely abolished, consistent with previous observations (Vanneste *et al.*, 2009). Together these results show that overexpressed GFP-Kif15 is distributed in a manner similar to that of the endogenous protein and that TPX2, but not kinetochore fibers, is required for spindle localization.

To examine Kif15-dependent spindle formation in LLC-Pk1 GFP-Kif15 cells, we first treated parental and GFP-Kif15 cells with 1 μM *S*-trityl-L-cysteine (STLC; DeBonis *et al.*, 2004) for 18 h and quantified

spindle morphology (Figure 3D). In parental cells treated with STLC, 96% of spindles were monopolar. In STLC-treated GFP-Kif15 cells, the majority of spindles were bipolar (87%), demonstrating that GFP-Kif15 can support bipolar spindle formation in these cells, consistent with results in other mammalian cells either overexpressing Kif15 or treated to develop resistance to STLC (Vanneste *et al.*, 2009; Raaijmakers *et al.*, 2012; Sturgill and Ohi, 2013; Sturgill *et al.*, 2016). Next we assessed the ability of STLC-treated, GFP-Kif15–expressing cells to form bipolar spindles after siRNA-mediated depletion of TPX2. As shown in Figure 3D, 97% of spindles were monopolar, indicating that TPX2 is required for Kif15-dependent bipolar spindle formation (Tanenbaum *et al.*, 2009). It should be noted, however, that depletion of TPX2 in control cells also leads to defects in spindle formation, resulting in short bipolar spindles, multipolar spindles, and monopolar spindles (Gruss and Vernos, 2004)

Because our data showed that the C-terminal 37 amino acids of TPX2 are important for spindle localization of Kif15 and inhibition of Kif15 motility in vitro, we next used cell lines expressing full-length or truncated TPX2 from a BAC to determine whether the C-terminal region is important for force generation by Kif15 in vivo. Cells were co-nucleofected with siRNA to deplete endogenous TPX2 and with a plasmid encoding mCherry-Kif15. At 40 h after nucleofection, cells were treated with STLC and spindle morphology scored. As shown in Figure 3D, bipolar spindles were present in the majority of cells expressing full-length TPX2 but not in cells expressing TPX2-710. This result demonstrates that the C-terminal region of TPX2 is necessary for Eg5-independent bipolar spindle formation in cells overexpressing Kif15.

The mechanism by which Kif15 promotes spindle bipolarity in the absence of Eg5 activity is not known but has been proposed to result from Kif15 action on parallel, bundled microtubules (Sturgill and Ohi, 2013). Consistent with this, recent work shows that some kinesin-5 inhibitor–resistant cell lines express low levels of a rigor mutant of Eg5 that promotes microtubule bundle formation (Sturgill *et al.*, 2016). To determine whether microtubule bundles are sufficient for Kif15 localization in the absence of TPX2, we depleted cells of TPX2 and added 2-[1-(4-fluorophenyl)cyclopropyl]-4-(pyridin-4-yl) thiazole (FCPT), which induces microtubule bundle formation by promoting rigor binding of Eg5 to microtubules (Groen *et al.*, 2008). Treatment of parental cells with FCPT alone promoted microtubule bundle formation as expected; however, very few bundles were observed in the absence of TPX2 (Figure 3E). Immunostaining showed that Eg5 bound to microtubule bundles in FCPT-treated cells, was reduced in siTPX2-treated cells, and bound to residual bundles in cells treated with both FCPT and siRNA to TPX2 (Figure 3E). Although Kif15 was detected on bundles in FCPT-treated cells, it was not detected in cells treated with siRNA targeting TPX2, even when FCPT was added to promote bundle formation (Figure 3E). These results show that Eg5 can bind to spindle microtubules in the absence of TPX2 when rigor binding of Eg5 to microtubules is promoted by FCPT treatment. However, in cells lacking TPX2, the formation of microtubule bundles using FCPT treatment alone may not be sufficient to localize Kif15 properly to the spindle.

Dynamic microtubules contribute to Kif15 behavior in vivo

Although Kif15 motility in vitro has been characterized (Drechsler *et al.*, 2014; Sturgill *et al.*, 2014), the motile behavior of Kif15 in vivo has not been reported. To investigate this, we performed time-lapse confocal microscopy of GFP-Kif15–expressing LLC-Pk1 cells, which remain relatively flattened during mitosis, facilitating imaging. We observed rapid motion of fluorescent particles of GFP-Kif15 toward the spindle equator, where microtubule plus ends are located (Figure 4A and Supplemental Movies S1 and S2). Close inspection of the confocal image sequences revealed some variation in the fluorescence intensity and morphology of the motile particles (Figure 4, A and D, and Supplemental Movie S1). The larger or brighter particles may represent clusters of Kif15 tetramers, a possibility that is consistent with recent in vitro experiments that show accumulation of Kif15 at intersections of dynamic microtubules and at microtubule plus ends (Dreschler and McAinsh, 2016). However, the fluorescent puncta move rapidly and photobleach quickly, so variation in morphology of individual puncta could not be quantified. When cells progressed into anaphase, GFP-Kif15 was enriched along kinetochore fibers and in some cases showed an accumulation near kinetochore fiber plus ends (Figure 4B and Supplemental Figure S3B).

We also performed TIRF microscopy of live cells to visualize motors on microtubules that extended to the peripheral regions of the cell (Gable *et al.*, 2012). In accord with results from confocal microscopy, GFP-Kif15 motors appeared to move in a directed manner, away from the centrosome, consistent with predominantly plus end–directed motion (Supplemental Figure S3A).

To determine whether the fluorescent particles of GFP-Kif15 are walking along the lattice of spindle microtubules or moving with the tips of growing microtubules, we measured the velocity of GFP-Kif15 in vivo from kymographs (Figure 4C) of fluorescent particles in the image sequences taken of metaphase and anaphase cells (*Materials and Methods*). We also imaged LLC-Pk1 cells expressing GFP-EB1, using identical imaging parameters, to determine the rate of microtubule growth (Piehl *et al.*, 2004). This analysis showed that particles of GFP-Kif15 moved in a processive manner at a velocity of 133 ± 43 nm/s. This value was not different from the rate of microtubule growth determined from the GFP-EB1 movies, 119 ± 26 nm/s ($p = 0.09$) suggesting that Kif15 motility results from association with growing microtubule ends. We also imaged both GFP-Kif15 and GFP-EB1 at room temperature, which reduced photobleaching, and again found that the velocities were not different (unpublished data). The relatively wide distribution in the velocities of GFP-Kif15 puncta could reflect different rates for single or multiple motors, for motors walking on one microtubule with a second microtubule as cargo, or because some motors are moving on microtubule growing ends and others are walking along the microtubule lattice (Dreschler and McAinsh, 2016). To determine whether this motile behavior is unique to GFP-Kif15, we overexpressed Eg5-Emerald from a plasmid and imaged the cells. In this case, plus end–directed motile behavior was not observed (unpublished data), consistent with previous work demonstrating that Eg5, expressed from a BAC, bound and unbound rapidly from mitotic microtubules and showed dynein-dependent minus-end motion (Uteng *et al.*, 2008; Gable *et al.*, 2012).

To determine whether GFP-Kif15 motility results from motors associating with dynamic microtubule plus ends (Dreschler and McAinsh, 2016), we treated GFP-Kif15 cells with nanomolar concentrations of paclitaxel to suppress microtubule dynamics (Yvon *et al.*, 1999). Under these conditions (*Materials and Methods*), the velocity and number of growing microtubule plus ends measured in GFP-EB1–expressing LLC-Pk1 cells was reduced, confirming a suppression of microtubule dynamics (Supplemental Figure S3, C and D). Time-lapse movies of paclitaxel-treated GFP-Kif15 cells showed a dramatic reduction of Kif15 motility on the spindle, which precluded tracking. This result shows that microtubule dynamics contributes to GFP-Kif15 behavior in vivo (Figure 4D and Supplemental Movie S3). Because of the high density of microtubules in the spindle and the fact that the Kif15 antibody is compatible only with methanol-fixed

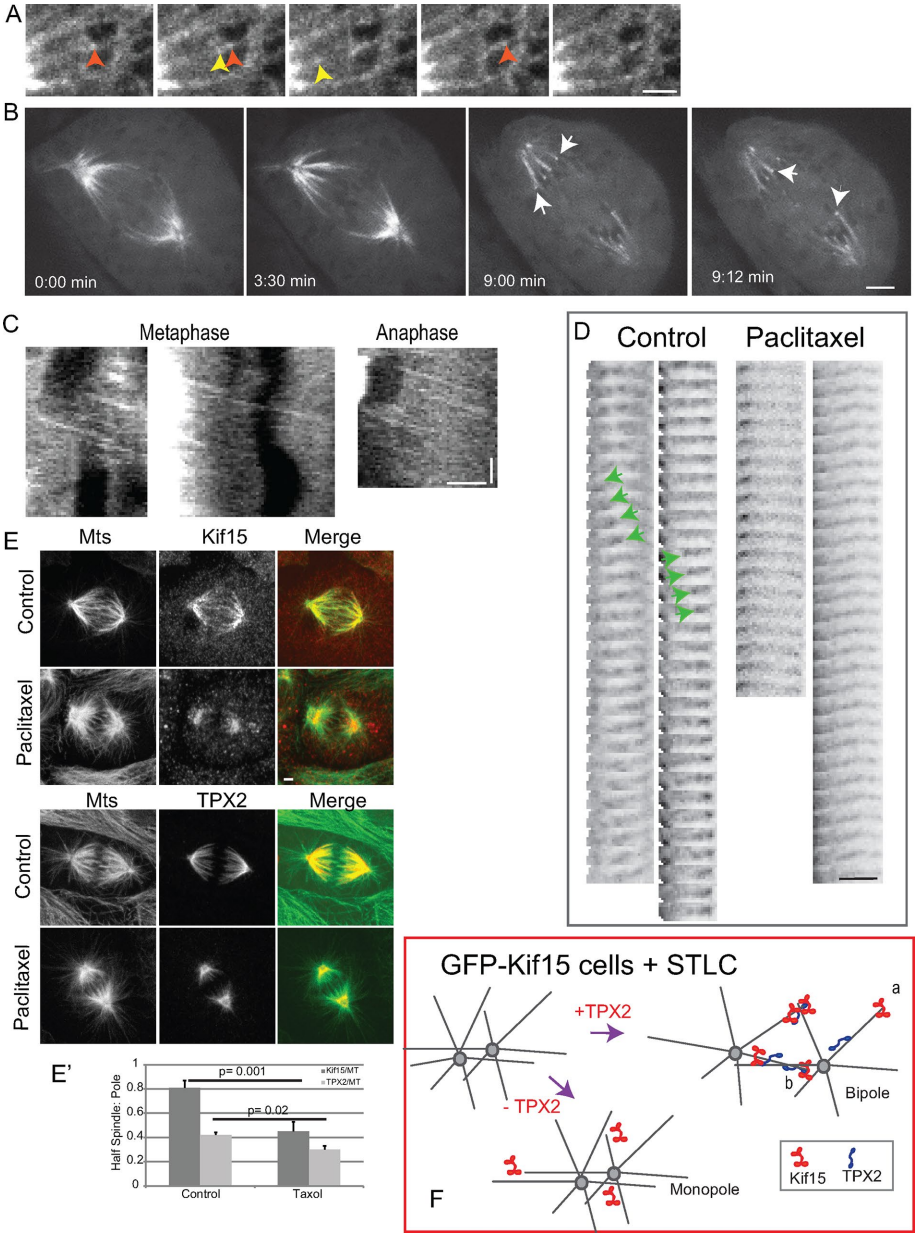

FIGURE 4: Dynamics of GFP-Kif15 in vivo. (A) Selected frames from a movie of GFP-Kif15–expressing cells; red and yellow arrowheads mark fluorescent particles traveling toward the chromosome region (spindle equator to the right; dark ovals are chromosomes). (B) Live cell expressing GFP-Kif15 progressing from prometaphase (0:00) to metaphase (3:30) and anaphase (9:00); arrows show accumulation of fluorescence near the kinetochores. (C) Kymographs from movie sequences of GFP-Kif15–expressing metaphase and anaphase cells; distance, horizontal axis; time, vertical axis; dark regions are chromosomes; spindle midzone to right. (D) Sequential frames (2-s interval) from movies of GFP-Kif15–expressing control and paclitaxel-treated cells (inverted contrast); motion of fluorescent particles toward the kinetochore region (right) in control but not paclitaxel-treated cells. Green arrowheads mark moving puncta. (E) LLC-Pk1 parental cells fixed and stained for microtubules and Kif15 (top) or TPX2 (bottom); control and paclitaxel as indicated; merged images to the right. (E') Bar graph showing quantification of images in E. (F) Cartoon showing GFP-Kif15 cells in the presence of STLC; bipolar spindle formation requires TPX2. TPX2 could load Kif15 onto the microtubule, followed by motor motion to the microtubule plus end (a), or TPX2 and Kif15 could both localize to microtubule ends (b). Bars, 2 μm (A–E); time scale, 30 s (C).

cells, we were not able to document colocalization of Kif15 and GFP-EB1 in fixed cells, and in live cells, expression of both GFP-Kif15 and mCherry-EB1 resulted in aberrant spindle morphology.

To determine whether the distribution of Kif15 and TPX2 was altered in paclitaxel-treated cells, as might be expected if the motors preferentially associate with dynamic microtubules, we fixed parental cells and stained them for microtubules and TPX2 or Kif15. The results show that suppression of dynamics with paclitaxel resulted in an increase in TPX2 and Kif15 near the spindle poles and a reduction along spindle microtubules (Figure 4E). To quantify this, we normalized TPX2 and Kif15 levels to tubulin and determined the ratio of each protein in the half-spindle and at the pole; the results show that paclitaxel treatment reduced this ratio for both Kif15 and TPX2 (Figure 4E'). This result shows that the distribution of TPX2 and Kif15 is affected by microtubule dynamics, consistent with the enrichment of TPX2 and Kif15 at plus ends of dynamic microtubules in vitro (Roostalu *et al.*, 2015; Dreschler and McAinsh, 2016; Reid *et al.*, 2016). Kif15 and TPX2 lack a short amino acid motif composed of serine, any amino acid, isoleucine, and proline (SxIP) that is commonly found in proteins that localize to microtubule plus ends in an EB-1–dependent manner (Honnappa *et al.*, 2009). This suggests that the association of TPX2 and Kif15 with microtubules is direct rather than mediated by EB1. TPX2 has been reported to associate with dynamic microtubule ends in vitro at low concentrations (Roostalu *et al.*, 2015; Reid *et al.*, 2016) but has not been reported to tip track in vivo, where it is present at higher concentrations (~20 nM in a mitotic cell extract). One possibility is that TPX2 is required to load Kif15 onto microtubules but not for it to remain at the growing plus end (Figure 4Fa); alternatively, TPX2 may remain at the plus end with Kif15 (Figure 4Fb) but not be detectable in vivo (Roostalu *et al.*, 2015; Dreschler and McAinsh, 2016; Reid *et al.*, 2016).

DISCUSSION

The results of these experiments demonstrate that the C-terminal region of TPX2, which was shown previously to contribute to the regulation of the kinesin-5, Eg5, also contributes to the regulation of the kinesin-12, Kif15. Specifically, the C-terminal 37 amino acids of TPX2 contribute to the spindle localization of each motor and inhibition of motor walking in vitro. In the case of Eg5, both TPX2-710 and full-length TPX2 had an inhibitory effect on motor stepping in vitro, although full-length TPX2 was a more effective inhibitor (Balchand *et al.*, 2015). This is in contrast to Kif15, which was inhibited only when the full-length protein was added. The reason for these differences is not clear; one possibility is that Eg5 is more susceptible to inhibition because of

differences in the neck linker and stalk, which are unique to Eg5 (Waitzman and Rice, 2014).

Our results showing that the C-terminal region of TPX2 contributes to the spindle localization of both Eg5 and Kif15, two kinesins that contribute to spindle bipolarity, raises the question of how bipolarity is achieved in cells expressing truncated TPX2. First, for both motors, spindle localization is reduced but not eliminated when TPX2-710 is expressed, which is consistent with the observation that the Eg5-TPX2 interaction is not completely abolished when the C-terminal region is removed from the protein (Eckerdt *et al.*, 2008; Ma *et al.*, 2011); the residual binding may be sufficient to generate bipolar spindles. In addition, incomplete knockdown of TPX2 may contribute to motor binding to spindle microtubules. Second, in LLC-Pk1 cells, centrosome separation typically occurs during prophase, when most of TPX2 is in the nucleus and thus before complete inhibition of Eg5 by TPX2 can occur (Raaijmakers *et al.*, 2012). Finally, it is possible that TPX2 also affects minus end–directed motility (Wittmann *et al.*, 1998) and that the reduction of both inward and outward force generators enables spindle bipolarization via microtubule-pushing forces (Wittmann *et al.*, 1998; Ferenz *et al.*, 2009; Toso *et al.*, 2009).

In Kif15-overexpressing cells treated with STLC, spindle formation is believed to occur when a monopolar spindle breaks symmetry, driven by Kif15 acting on parallel, bundled microtubules (Sturgill and Ohi, 2013; Sturgill *et al.*, 2014). When TPX2 is depleted from these cells, bipolar spindles are not observed (this study; Tanenbaum *et al.*, 2009). One possibility is that TPX2 is needed to generate microtubule bundles to which Kif15 binds (Sturgill *et al.*, 2014); alternatively, TPX2 may play a more direct role in promoting force generation by Kif15 (Drechsler *et al.*, 2014). Note that depletion of TPX2 results in a dramatic alteration of spindle morphology, resulting in short spindles with extensive astral arrays and few or no spindle microtubules (Gruss *et al.*, 2002), and these changes affect spindle formation. However, in Kif15-overexpressing cells expressing TPX2-710, microtubule formation in the chromosome pathway can proceed (Ma *et al.*, 2011), and these cells also fail to generate bipolar spindles. This suggests that TPX2 is needed not only to promote microtubule formation but also to regulate motor activity, which is consistent with in vitro experiments showing that the C-terminus of TPX2 is required for motor regulation on individual, unbundled, microtubules (this study) and experiments showing that Kif15 can generate greater force in the presence of TPX2 (Drechsler *et al.*, 2014).

Our analysis is the first report of the motile behavior of GFP-Kif15 on spindle microtubules in vivo. We observed plus end–directed motion of Kif15 puncta in prometaphase, metaphase, and anaphase cells. In live cells, Kif15 puncta moved at a rate (133 nm/s) that was indistinguishable from microtubule plus-end growth in these cells (119 nm/s) and was suppressed in cells treated with paclitaxel to reduce microtubule dynamics. These observations support the idea that motion of Kif15 is due, at least in part, to tracking with microtubule plus ends. This possibility is also consistent with in vitro experiments showing that Kif15 tracks, and accumulates at, the plus ends of dynamic microtubules, in the absence of other microtubule-associated proteins (Dreschler and McAinsh, 2016). The velocity of GFP-Kif15 puncta in live cells overlaps with the velocity of GFP-Kif15 measured in vitro on stable microtubules (~130 nm/s) but is slower than the velocity on dynamic microtubules (~500 nm/s; Dreschler and McAinsh, 2016). Because microtubules in vivo are highly dynamic, the velocity of Kif15 in vivo is predicted to be ~500 nm/s (Verhey *et al.*, 2011). The similarity of the velocities of microtubule growth and Kif15 puncta motility is thus consistent with motors tracking plus ends, but we cannot eliminate the possibility that Kif15 walking on spindle microtubules in vivo also contributes to the observed motility. Because puncta composed of multiple tetramers of GFP-Kif15 are easier to detect in live cells, our imaging experiments may preferentially capture the brighter puncta at microtubule ends, and individual motors on the microtubule lattice may be insufficiently bright to track. Note that measuring the rate that a mitotic motor walks in vivo is challenging. In the case of Eg5, prior work showed that motors bound and unbound rapidly to spindle microtubules (Gable *et al.*, 2012). In the interzonal region, short excursions were measured with a rate of ~6.5 nm/s, similar to the rate that Eg5 walks in vitro (Weinger *et al.*, 2011; Balchand *et al.*, 2015). In contrast, in the half-spindle, Eg5 moved toward the spindle poles in a dynein-dependent manner (Uteng *et al.*, 2008; Gable *et al.*, 2012). To our knowledge, the in vivo motile behavior of individual molecules of other mammalian mitotic motors has not been reported. Therefore additional experiments are required to establish whether Kif15 walks on the microtubule lattice, tracks the microtubule plus end, or both in vivo (Dreschler and McAinsh, 2016).

We observed Kif15 puncta on kinetochore fibers in fixed and live cells, consistent with the fact that Kif15 can cross-link parallel microtubules in vitro (Drechsler *et al.*, 2014; Sturgill *et al.*, 2014). One appealing possibility is that Kif15 can aid in the formation of parallel microtubule bundles in the spindle by walking along a kinetochore microtubule while associated with a dynamic growing microtubule. In late anaphase and telophase cells, Kif15 was not detected on overlapping interzonal microtubules, consistent with preferential binding to parallel microtubules.

Mitotic motors, including Eg5 and Kif15, and TPX2 are all subject to mitotic regulation (Blangy *et al.*, 1997; Nousiainen *et al.*, 2006; Fu *et al.*, 2015; vanHeesbeen *et al.*, 2016) but how these modifications affect motor behavior in vitro and in vivo is incompletely understood. For example, modifications of mitotic motors regulate their binding to spindle microtubules as cells enter mitosis, but it is not known whether these modifications also affect their interaction with TPX2. In addition, it has not been determined whether there is competition between these motors for interaction with TPX2. Enrichment of GFP-Kif15 on kinetochore fibers was observed as cells progressed into anaphase, suggesting that Kif15 distribution and function may change not only as cells enter mitosis, but also as cells progress into anaphase.

In conclusion, the results of these in vitro experiments show that Kif15 is a processive, track-switching motor and that a fraction of the motors exist as tetramers in both interphase and mitotic extracts, supporting the view that Kif15, like Eg5, functions as a tetramer. The results presented here demonstrate that the C-terminal 37 amino acids of TPX2 regulate in vitro motility of Kif15 and contribute to the spindle localization of Kif15 and Eg5-independent force generation by Kif15 in vivo. Our live-cell imaging shows that Kif15 moves in a manner consistent with tracking microtubule plus ends in vivo, which likely aids the motor aligning microtubules into kinetochore fibers and generating force for bipolarization. Together with other work, our results highlight the essential role of microtubule-associated proteins in regulating the cellular activity of kinesin motors (Dixit *et al.*, 2008; Wignall and Villeneuve, 2009; Barlan *et al.*, 2013; Li *et al.*, 2016).

MATERIALS AND METHODS

Materials

All chemicals, unless otherwise specified, were purchased from Sigma-Aldrich.

Cell culture, nucleofection, and inhibitor treatments

LLC-Pk1 cells were cultured in a 1:1 mixture of F10 Ham's and Opti-MEM containing 7.5% fetal bovine serum and antibiotics and maintained at 37°C and 5% CO_2. LLC-Pk1 cells were nucleofected using an Amaxa Nucleofector (Lonza, Basel, Switzerland) using program X-001 and Mirus nucleofection reagent (Mirus Bio, Madison, WI) according to the manufacturers' recommendations. The following siRNAs were used: TPX2, GGACAAAACUCCUCUGAGA; Nuf2, AAGCAUGCCGUGAAACGUAUA; and Kif15, UGACAUCACUUGCAAAUAC. siRNAs were purchased from Dharmacon (GE Healthcare Life Sciences, Pittsburgh, PA).

LLC-Pk1 cells expressing full-length TPX2 or TPX2-710 from a BAC were grown as previously described (Ma *et al.*, 2011). To generate cells expressing GFP-Kif15, parental cells were nucleofected with GFP-Kif15 and selected using the appropriate antibiotic; cells were subcloned to enrich for GFP-Kif15–expressing cells. For some experiments, GFP-Kif15 cells that had been further selected for fluorescence using cell sorting were used. mCherry-Kif15 was prepared by subcloning of GFP-Kif15 into the appropriate vector.

Paclitaxel, FCPT, and STLC were prepared as stock solutions in dimethyl sulfoxide, stored at –20°C, and diluted with culture medium before use. FCPT was used at 200 µM, paclitaxel at 330 nM, and STLC at 1 µM.

Preparation of cell extracts

Cell extracts for TIRF experiments were prepared from LLC-Pk1 cells expressing GFP-Kif15. A confluent 100-mm-diameter cell culture dish was washed twice with calcium and magnesium-free phosphate-buffered saline (PBS), and then 300 µl of extraction buffer (40 mM 4-(2-hydroxyethyl)-1-piperazineethanesulfonic acid/KOH, pH 7.6, 100 mM NaCl, 1 mM EDTA, 1 mM phenylmethylsulfonyl fluoride, 10 µg/ml leupeptin, 1 mg/ml pepstatin, 0.5% Triton X-100, and 1 mM ATP) was added dropwise to the dish and incubated with gentle rotation for ~2 min (Cai *et al.*, 2007; Balchand *et al.*, 2015). The extract was transferred to a microcentrifuge tube on ice and centrifuged at 15,000 rpm at 4°C for 10 min in a tabletop centrifuge. The supernatant was recovered and used immediately or stored in aliquots in liquid nitrogen; protein concentration was determined using the method of Lowry *et al.* (1951). For quantification of the fluorescence intensity of individual puncta using TIRF microscopy, the cells were treated with siRNA targeting endogenous Kif15 72 h before preparation of the extract.

To prepare mitotic extracts, GFP-Kif15 cells were treated with siRNA targeting endogenous Kif15 and synchronized using 330 nM nocodazole for the final 18 h of the 72-h siRNA treatment. Extracts were prepared as described, with the addition of Simple Stop 1 Phosphatase Inhibitor Cocktail (1X; Gold Biotechnology, St. Louis, MO) to the extract buffer.

Protein purification

Full-length and truncated TPX2 were expressed and purified from bacteria as previously described (Balchand *et al.*, 2015). Kinesin-1–GFP was prepared using the dimeric construct as previously described (Balchand *et al.*, 2015). To generate TPX2-657, a stop codon was introduced at amino acid 657 in the bacterially expressed full-length TPX2 construct. To generate TPX2-ΔPFAM, PCR was used to remove amino acids 662–719 from full-length TPX2. Proteins were run on 8% polyacrylamide gels using appropriate molecular weight standards and stained with Coomassie brilliant blue.

Single-molecule experiments

For the single-molecule experiments, perfusion chambers (~10-µl volume) were made from glass slides, silanized coverslips, and double-stick tape (Balchand *et al.*, 2015). First, 10 µl of 10% rat YL ½ anti-tubulin antibody (Accurate Chemical and Scientific) was flowed into the chamber and incubated for 3 min. Next the chamber was blocked by flowing in 5% Pluronic F-127 for 3 min. Diluted rhodamine-labeled microtubules composed of 10% rhodamine tubulin (Cytoskeleton) and unlabeled porcine brain tubulin were flowed into the chamber and incubated for 3 min, followed by a second block of 5% Pluronic F-127. Cell extract containing GFP-Kif15 was diluted in PEM 20 motility buffer (20 mM 1,4-piperazinediethanesulfonic acid, pH 6.9, 2 mM ethylene glycol tetraacetic acid, 2 mM $MgSO_4$) containing 0.25% F127, 100 µM ATP, 1 mM dithiothreitol, and 25 µM paclitaxel and supplemented with an oxygen-scavenging system (15 mg/ml glucose, 1.23 mg/ml glucose oxidase, and 0.375 mg/ml catalase), flowed into the chamber, and imaged. To determine the directionality of Kif15, polarity-marked microtubules were used, and it was confirmed that Kif15 walked toward the plus end for the majority of excursions. For preincubation experiments with TPX2, the indicated concentrations of TPX2 were added to the motility buffer containing GFP-Kif15 and incubated on ice for 2 min before flowing into the chamber. Single-molecule imaging of kinesin-1–GFP was performed as described previously (Balchand *et al.*, 2015).

Microscope imaging and analysis

TIRF microscopy was performed using a Nikon (Melville, NY) Ti-E microscope with a 100×/1.49 numerical aperture (NA) objective lens and an Andor (Belfast, UK) Zyla scientific complementary metal-oxide semiconductor camera; the system was run by Nikon Elements software. TIRF imaging was performed at room temperature; images were collected at 1 frame/s for a total of 300 s. To measure motor velocity, individual puncta were tracked using the Particle Tracking function of Nikon Elements software and exported to Excel for analysis. For the experiment with mitotic extract, a Nikon Ti-E microscope run by MetaMorph software and with a Hamamatsu Flash 4.0 camera was used.

Live and fixed cells were imaged using either spinning-disk confocal microscopy or point-scanning confocal microscopy. For spinning-disk confocal microscopy, two different systems were used, either a Nikon Ti-E microscope with a CSU-X1 Yokogawa spinning-disk confocal scan head (PerkinElmer, Wellesley, MA), an Andor iXon+ electron-multiplying charge-coupled device camera (Andor), and a 100×/1.4 NA objective lens or a CSU-10 Yokogawa spinning-disk confocal microscope on a Nikon TE300 as previously described (Tulu *et al.*, 2003). For live-cell imaging, exposures were adjusted without saturating the camera's pixels; typical exposures were 50–800 ms. For point-scanning confocal microscopy, a Nikon A1R system with a 60×/1.4 NA objective lens was used. Images of live cells were acquired every 2 s at room temperature or every 3 s at ~34°C; images were typically collected for 2–5 min. For both fixed- and live-cell imaging, a laser power of 1–2% was used. For heating the cells during imaging, a Nicholson Precision Instruments (Bethesda, MD) Air Stream Stage Incubator was used; temperature was measured using a thermistor probe taped to the microscope stage outside of the cell chamber. When the thermistor temperature is 37°C, the temperature inside the chamber is ~34°C.

To quantify the fluorescence intensity of tubulin and Kif15, a 1 × 1 µm box was placed midway between the spindle pole and the chromosomes or at the spindle pole, and the ratio of Kif15 to tubulin fluorescence was measured after background subtraction. Statistical analysis was performed in Excel. Velocity of GFP-EB1

dashes and Kif15 puncta were tracked in ImageJ using the M Track J plug-in.

Immunofluorescence

LLC-Pk1 cells were plated on #1.5 glass coverslips ~48 h before experiments. For Kif15 staining, cells were rinsed twice with room temperature PBS lacking calcium and magnesium, fixed in –20°C methanol for 5–10 min, and rehydrated in PBS containing 0.1% Tween and 0.02% sodium azide (PBS-Tw-Az). Kif15 primary antibodies (Cytoskeleton, Denver, CO) were used following the manufacturer's recommendation and subsequently stained with fluorescent secondary anti-rabbit antibodies (Ma *et al.*, 2011). For TPX2 staining, cells were fixed in 2% paraformaldehyde, 0.25% glutaraldehyde, and 0.5% Triton X-100 made fresh daily in PBS lacking calcium and magnesium. TPX2 antibodies were obtained from Novus Biologicals (Littleton, CO); Hec1 antibodies (Abcam, Cambridge, MA) were the kind gift of T. Maresca (University of Massachusetts). Microtubules were stained with either DM1a mouse anti-tubulin (Sigma Chemical Co.) or YL1/2 rat anti-tubulin (Accurate Chemical and Scientific, Westbury, NY) and appropriate secondary antibodies as previously described (Ma *et al.*, 2011). Stained cells were mounted on glass slides using Fluomount G (Southern Biotech, Birmingham, AL) to which 4′,6-diamidino-2-phenylindole was added to stain DNA.

Western blotting and detection

Whole-cell extracts of control or siRNA-treated cells were prepared by adding SDS sample buffer to 35-mm dishes of cells, followed by sonication. Extracts were run on 8% SDS polyacrylamide gels using the formulation of Laemmli (1970). Gels were transferred onto Amersham Hybond-P membrane (GE Healthcare, Waukesha, WI). Blots were probed with Kif15 or TPX2 antibodies used at 1:1000 for 1 h at room temperature in 5% nonfat dry milk dissolved in Tris-buffered saline containing 0.02% Tween-20 (TBS-Tween). The blots were then probed with goat anti-rabbit horseradish peroxidase–conjugated secondary antibody (1:5000; Jackson ImmunoResearch Laboratories, West Grove, PA) for 1 h at room temperature in 5% nonfat dry milk dissolved in TBS-Tween and detected using chemiluminescence.

ACKNOWLEDGMENTS

We thank I. Vernos for the kind gift of a plasmid encoding GFP-Kif15, Andrew McAinsh and members of the Maresca and Lee labs, University of Massachusetts, for fruitful discussions and commentary, Heather Jordan for assistance with Western blots, Brett Estes for quantification of images, and Aishwarya Vishwanath for measuring the cellular level of TPX2.

REFERENCES

Balchand SK, Mann BJ, Titus J, Ross JL, Wadsworth P (2015). TPX2 inhibits Eg5 by interactions with both motor and microtubule. J Biol Chem 290, 17367–17379.

Barlan K, Lu W, Gelfand VI (2013). The microtubule-binding protein ensconsin is an essential cofactor of kinesin-1. Curr Biol 23, 317–322.

Blangy A, Arnaud L, Nigg EA (1997). Phosphorylation by $p34^{cdc2}$ protein kinase regulates binding of the kinesin related motor HsEg5 to the dynactin subunit $p150^{glued}$. J Biol Chem 272, 19418–19424.

Blangy A, Lane HA, d'Herin P, Harper M, Kress M, Nigg EA (1995). Phosphorylation by $p34^{cdc2}$ regulates spindle association of human Eg5, a kinesin related motor essential for bipolar spindle formation in vivo. Cell 83, 1159–1169.

Brunet S, Sardon T, Zimmerman T, Wittman T, Pepperkok R, Karsenti E, Vernos I (2004). Characterization of the TPX2 domains involved in microtubule nucleation and spindle assembly in Xenopus egg extracts. Mol Biol Cell 15, 5318–5328.

Cai D, Verhey KJ, Meyhofer E (2007). Tracking single kinesin molecules in the cytoplasm of mammalian cells. Biophys J 92, 4137–4144.

DeBonis S, Skoufias DA, Lebeau L, Lopez R, Robin G, Margolis RL, Wade RH, Kozielski F (2004). In vitro screening for inhibitors of the human mitotic kinesin Eg5 with antimitotic and antitumor activities. Mol Cancer Ther 3, 1079–1090.

Dixit R, Ross JL, Goldman YE, Holzbaur EL (2008). Differential regulation of dynein and kinesin motor proteins by Tau. Science 319, 1086–1089.

Dreschler H, McAinsh AD (2016). Kinesin-12 motors cooperate to suppress microtubule catastrophes and drive the formation of parallel microtubule bundles. Proc Natl Acad Sci USA 113, E1635–E1644.

Drechsler H, McHugh T, Singleton MR, Carter NJ, McAinsh AD (2014). The kinesin-12 Kif15 is a processive track-switching tetramer. Elife 3, e01724.

Eckerdt F, Eyers PA, Lewellyn AL, Prigent C, Maller JL (2008). Spindle pole regulation by a discrete Eg5-interacting domain in TPX2. Curr Biol 18, 519–525.

Ferenz N, Paul R, Fagerstrom C, Mogilner A, Wadsworth P (2009). Dynein antagonizes Eg5 by crosslinking and sliding antiparallel microtubules. Curr Biol 19, 1833–1838.

Ferenz NP, Gable A, Wadsworth P (2010). Mitotic functions of kinesin-5. Semin Cell Dev Biol 21, 255–259.

Fu J, Bian M, Xin G, Deng Z, Luo J, Guo X, Chen H, Wang Y, Jiang Q, Zhang C (2015). TPX2 phosphorylation maintains metaphase spindle length by regulating microtubule flux. J Cell Biol 210, 373–383.

Gable A, Qiu M, Titus J, Balchand S, Ferenz NP, Ma N, Fagerstrom C, Ross JL, Yang G, Wadsworth P (2012). Dynamic reorganization of Eg5 in the mammalian spindle throughout mitosis requires dynein and TPX2. Mol Biol Cell 23, 1254–1266.

Groen AC, Needleman D, Brangwynne C, Gradinaru C, Fowler B, Mazitschek R, Mitchison TJ (2008). A novel small-molecule inhibitor reveals a possible role of kinesin-5 in anastral spindle-pole assembly. J Cell Sci 121, 2293–2300.

Gruss OJ, Vernos I (2004). The mechanism of spindle assembly: functions of Ran and its target TPX2. J Cell Biol 166, 949–955.

Gruss OJ, Wittmann M, Yokoyama H, Pepperkok R, Kufer T, Sillje H, Karsenti E, Mattaj IW, Vernos I (2002). Chromosome-induced microtubule assembly mediated by TPX2 is required for spindle formation in HeLa cells. Nat Cell Biol 4, 871–879.

Honnappa S, Gouveia SM, Weisbrich A, Damberger FF, Bhavesh NS, Jawhari H, Grigoriev I, van Rijssel FJA, Buey RM, Lawera A, *et al.* (2009). An EB1-binding motif acts as a microtubule tip localization signal. Cell 138, 366–376.

Kalab P, Pralle A, Isacoff EY, Weis K (2006). Analysis of a RanGTP-regulated gradient in mitotic somatic cells. Nature 440, 697–701.

Kapitein LC, Peterman EJG, Kwok BH, Kim JH, Kapoor TM, Schmidt CF (2005). The bipolar mitotic kinesin Eg5 moves on both microtubles that it crosslinks. Nature 435, 114–118.

Laemmli UK (1970). Cleavage of structural proteins during the assembly of the head of bacteriophase T4. Nature 227, 680–685.

Li C, Zhang Y, Yang Q, Ye F, Sun SY, Chen ES, Liou YC (2016). NuSAP modulates the dynamics of kinetochore microtubules by attenuating MCAK depolymerization activity. Sci Rep 6, 18773.

Lowry OH, Rosenbrough NJ, Farr AL, Randall RJ (1951). Protein measurement with the Folin phenol reagent. J Biol Chem 193, 265–275.

Ma N, Titus J, Gable A, Ross JL, Wadsworth P (2011). TPX2 regulates the localization and activity of Eg5 in the mammalian mitotic spindle. J Cell Biol 195, 87–98.

Meunier S, Vernos I (2016). Acentrosomal microtubule assembly in mitosis: the where, when and how. Trends Cell Biol 26, 80–87.

Nousiainen M, Sillje HHW, Sauer G, Nigg EA, Korner R (2006). Phosphoproteome analysis of the human mitotic spindle. Proc Natl Acad Sci USA 103, 5391–5396.

O'Connell CB, Loncarek J, Kalab P, Khodjakov A (2009). Relative contributions of chromatin and kinetochores to mitotic spindle assembly. J Cell Biol 187, 43–51.

Piehl M, Tulu US, Wadsworth P, Cassimeris L (2004). Centrosome maturation: measurement of microtubule nucleation throughout the cell cycle using GFP tagged EB1. Proc Natl Acad Sci USA 101, 1584–1588.

Raaijmakers JA, van Heesbeen RG, Meaders JL, Geers EF, Fernandez-Garcia B, Medema RH, Tanenbaum ME (2012). Nuclear envelope-associated dynein drives prophase centrosome separation and enables Eg5-independent bipolar spindle formation. EMBO J 31, 4179–4190.

Reid TA, Schuster BM, Mann BJ, Balchand SK, Plooster M, McClellan M, Coombes CE, Wadsworth P, Gardner MK (2016). Suppression of microtubule assembly kinetics by the mitotic protein TPX2. J Cell Sci 129, 1319–1328.

Roostalu J, Cade NI, Surrey T (2015). Complementary activities of TPX2 and chTOG constitute an efficient importin-rregulated microtubule nucleation module. Nat Cell Biol 17, 1422–1437.
Sturgill EG, Das DK, Takizawa Y, Shin Y, Collier SE, Ohi MD, Hwang W, Lang MJ, Ohi R (2014). Kinesin-12 Kif15 targets kinetochore fibers through an intrinsic two-step mechanism. Curr Biol 24, 2307–2313.
Sturgill EG, Norris SR, Guo Y, Ohi R (2016). Kinesin-5 inhibitor resistance is driven by kinesin-12. J Cell Biol 213, 213–227.
Sturgill EG, Ohi R (2013). Kinesin-12 differentially affects spindle assembly depending on its microtubule substrate. Curr Biol 23, 1280–1290.
Tanenbaum ME, Macurek L, Jeanssen N, Geers EF, Alvarez-Fernandez M, Medema RH (2009). Kif15 cooperates with Eg5 to promote bipolar spindle assembly. Curr Biol 19, 1–9.
Toso A, Winter JR, Garrod AJ, Amaro AC, Meraldi P, McAinsh AD (2009). Kinetochore-generated pushing forces separate centrosomes during bipolar spindle assembly. J Cell Biol 184, 365–372.
Tulu US, Fagerstrom C, Ferenz NP, Wadsworth P (2006). Molecular requirements for kinetochore-associated microtubule formation in mammalian cells. Curr Biol 16, 536–541.
Tulu US, Rusan N, Wadsworth P (2003). Peripheral, noncentrosome-associated microtubules contribute to spindle formation in centrosome containing cells. Curr Biol 13, 1894–1899.
Uteng M, Hentrich C, Bieling P, Surrey T (2008). Poleward transport of Eg5 by dynein-dynactin in Xenopus egg extract spindles. J Cell Biol 182, 715–726.
vanHeesbeen RG, Raaijmakers JA, Tanenbaum ME, Halim VA, Lelieveld D, Lieftink C, Heck AJ, Egan DA, Medema RH (2016). Aurora A, MCAK, and Kif18b promote Eg5-independent spindle formation. Chromosoma 125, 1–14.
Vanneste D, Takagi M, Imamoto N, Vernos I (2009). The role of Hklp2 in the stabilization and maintenance of spindle bipolarity. Curr Biol 19, 1712–1717.
Verhey KJ, Kaul N, Soppina V (2011). Kinesin assembly and movement in cells. Annu Rev Biophys 40, 267–288.
Waitzman JS, Rice SE (2014). Mechanism and regulation of kinesin-5, an essential motor for the mitotic spindle. Biol Cell 106, 1–12.
Weinger JS, Qiu M, Yang G, Kapoor TM (2011). A nonmotor microtubule binding site in kinesin-5 is required for filament crosslinking and sliding. Curr Biol 21, 154–160.
Wignall SM, Villeneuve AM (2009). Lateral microtubule bundles promote chromosome alignment during acentrosomal oocyte meiosis. Nat Cell Biol 11, 839–844.
Wittmann T, Boleti H, Antony C, Karsenti E, Vernos I (1998). Localization of the kinesin-like protein Xklp2 to spindle poles requires a leucine zipper, a microtubule-associated protein and dynein. J Cell Biol 143, 673–685.
Wittmann T, Wilm M, Karsenti E, Vernos I (2000). TPX2, a novel Xenopus MAP involved in spindle pole organization. J Cell Biol 149, 1405–1418.
Yvon AC, Wadsworth P, Jordan MA (1999). Taxol suppresses dynamics of individual microtubules in living human tumor cells. Mol Biol Cell 10, 947–959.